

Predicting Soil Erosion With RUSLE in Mediterranean Agricultural Systems at Catchment Scale

Manuel López-Vicente and Ana Navas

Dept. of Soil and Water, Experimental Station of Aula Dei. Postal Box 13034, 50080 Zaragoza, Spain.

Fax: 34 976 716 145; E-mail: mlopezvicente@gmail.com; anavas@eead.csic.es

Corresponding author: Phone: +34 976 716 158; E-mail: mlopezvicente@gmail.com

Abstract: Accurate assessment of soil loss is essential for sustainable agricultural production, management and conservation planning, especially in productive rain-fed agro-ecosystems and protected areas. The European Union considers soil as a non-renewable resource and identifies that soil degradation has strong impacts on soil and water resources. In this work the Revised Universal Soil Loss Equation model was applied within a geographic information system in the Estaña catchment (Spanish Pre-Pyrenees) as representative of a Mediterranean agro-ecosystem to elaborate a map of soil erosion at high spatial resolution (5 x 5 m of cell size). The soil erodibility factor (K) is calculated from three different approaches to evaluate the importance of spatial variations in soil texture, field infiltration measurements (K_{fs}) and amount of coarse fragments. The average value of estimated soil loss for the whole study area is $2.3 \text{ Mg ha}^{-1} \text{ yr}^{-1}$ and the highest rates are estimated in crops in steep areas ($5.8 \text{ Mg ha}^{-1} \text{ yr}^{-1}$) and trails ($18.7 \text{ Mg ha}^{-1} \text{ yr}^{-1}$). Cultivated soils with high soil erosion rates (higher than $8 \text{ Mg ha}^{-1} \text{ yr}^{-1}$) represent 20% of the cultivated area. The average value of soil loss in areas with human disturbances ($4.21 \text{ Mg ha}^{-1} \text{ yr}^{-1}$) is 4.4 times higher than that estimated for areas with natural vegetation ($0.96 \text{ Mg ha}^{-1} \text{ yr}^{-1}$). Field validation with ^{137}Cs shows that the estimated value of soil loss in barley fields with the K - K_{fs} -rocks factor improves the model predictions in comparison with those obtained with the K -texture and K - K_{fs} factors. The RUSLE model predicts a decrease in soil erosion in fields in accordance with the increase of the age of abandonment. Predicted values of soil erosion and measured soil organic matter and stoniness in old abandoned fields agree with those in areas of natural forest and indicate the recovery of the original conditions of the soil. Statistical analysis highlights that the C factor contributes most of the variability of the values of predicted soil erosion, the K and LS factors contribute in a similar way and the P factor contributes least to the variability of soil erosion. Cultivated soils developed over clay materials in high slope areas are the most susceptible to soil

35 degradation processes in comparison with soils developed over limestones in gentle and
36 medium slope areas. The recovery of terraces in steep fields and conservation of crop residues
37 are proposed as soil conservation practices to reduce the magnitude of soil loss in the study
38 area.

39

40 **Key words:** Soil erosion; soil erodibility; RUSLE; ^{137}Cs ; land uses; Mediterranean agro-
41 ecosystems

42

43 **INTRODUCTION**

44 Soil erosion is one of the main threats in productive croplands (de Paz et al., 2006; López-
45 Bermúdez, 1990) and a limiting factor for the sustainability of semiarid and sub-humid agro-
46 ecosystems in Spain and other Mediterranean countries that are subject to strong human
47 pressure (Navas et al., 2005). Mediterranean agro-ecosystems are complex landscape units
48 characterized by croplands intersected with patches of natural vegetation, intense land use
49 changes during the last decades including land abandonment, deforestation, overgrazing and
50 extensive agriculture that promote land degradation (Thornes, 2007). Mediterranean soil
51 surface characteristics present high spatial heterogeneity (Corbane et al., 2008) and generally
52 poor conditions (Navas et al., 2007). Values of rainfall erosivity and soil erodibility vary
53 significantly within the year in Mediterranean areas, especially at the end of the summer when
54 extreme storm events happen and in winter due to the freeze-thaw cycles that affect soil
55 structure (López-Vicente et al., 2008). Mediterranean landscapes are erosion-sensitive areas
56 with high and very high rates ($> 25 \text{ Mg ha}^{-1} \text{ yr}^{-1}$) of soil erosion in croplands (Sadiki et al.,
57 2007), irreversible in rills and gullies ($> 30 \text{ Mg ha}^{-1} \text{ yr}^{-1}$) (Desir and Marín, 2007) and low and
58 medium rates in areas with natural vegetation (Zuazo et al., 2004). Hence, the consideration
59 of spatial variations in soil parameters is necessary to improve soil erosion predictions at
60 catchment scale (Nisar Ahamed et al., 2000).

61 Climate change is increasing both the frequency of heavy rainfall events in Mediterranean
62 areas (e.g. Tapiador et al., 2007) and of extreme daily rainfall in spite of decrease in total
63 amount in Spain and other Mediterranean countries (Alpert et al., 2002). The significant
64 increase in the severity of drought identified from 1951 to 2000 in northeast Spain (Vicente-
65 Serrano and Cuadrat-Prats, 2007) had critical consequences in vegetation growing and its
66 protection role on soil surface against water erosion by rainfall splash and runoff. Moreover,
67 desertification enlargement is a serious and a possible imminent scenario in Mediterranean
68 landscapes (Kéfi et al., 2007).

69 Soil loss results in substantial on-site and off-site erosion problems that have strong impacts
70 on areas of common interest, such as food safety (loss of fertile soil), water resources, human
71 health, climate change and biodiversity protection. To tackle this problem the United Nations
72 celebrated the Convention to Combat Desertification (IISD, 2007) and the European Union
73 (EU) recently presented the soil protection and amending framework (COM, 2006) and
74 directive (EPC, 2004). Therefore, the accurate assessment of runoff volume and spatially
75 distributed mapping of soil erodibility and erosion is required to understand and quantify the
76 consequences of land use changes, and of interest for local, national and European policy
77 makers to preserve soil and water resources, especially in soil erosion-sensitive areas such as
78 the Mediterranean agricultural systems.

79 Empirical models are easy to use and low time-consuming and perform equally well as the
80 more complex distributed models (Jetten et al., 2003). Mapping soil erosion with empirical
81 models at continuous temporal scale and GIS techniques allow identifying areas with high
82 erosion rates (Bartsch et al., 2002). The empirical RUSLE model predicts the average annual
83 long-term rates of soil loss at plot and catchment scale (Renard et al., 1991). This model is the
84 most worldwide accepted empirical model and was specially designed for cultivated areas
85 (Renard et al., 1997). The RUSLE model has been used in different environments and under
86 different land uses and spatial scales (e.g. Lewis et al., 2005; Lufafa et al., 2003) and in
87 Mediterranean agro-ecosystems in France (Morschel et al., 2004), Spain (Tejada and
88 Gonzalez, 2006; Boellstorff and Benito, 2005) and Italy (Pelacani et al., 2008; Onori et al.,
89 2006). Calibration of the RUSLE factors to Mediterranean conditions was done in Greece
90 (Arhonditsis et al., 2002) and Palestine (Hammad et al., 2004) and validation of the estimated
91 rates with observed values of soil loss was done in natural conditions and rainfall simulations
92 at plot scale (Spaeth Jr. et al., 2003). However, few works of validation of the RUSLE model
93 has been done in a spatially distributed way in Mediterranean catchments.

94 This work aims to estimate soil erodibility and erosion rates in the Estaña catchment (Spanish
95 Pre-Pyrenees) as representative of the complex Mediterranean agro-ecosystems. To assess the
96 importance of infiltration properties and coarse fragments on soil erosion the soil erodibility
97 (K) factor is estimated following three different approaches. The accuracy of the different
98 approaches is evaluated with quantified rates of soil loss with ^{137}Cs at several control points in
99 crops of barley. In order to analyze the effect of human disturbances and physiographic
100 properties on soil erosion the annual values of predicted soil erosion are calculated for the
101 different land uses paying special attention in croplands and abandoned fields. This work is of
102 interest to assess the accuracy of three different approaches of soil erodibility as well as to

103 identify the main land uses causing erosion in the Estaña catchment and to propose soil
104 conservation practices that could be used in other Mediterranean agricultural systems to
105 promote best management practices (BMPs).

106

107 **MATERIALS AND METHODS**

108 **Study area**

109 The Estaña catchment is a medium-scale endorheic watershed (246 ha) that is located in the
110 External Ranges of the Central Spanish Pre-Pyrenees and elevation ranges between 676 and
111 896 m a.s.l. (Fig. 1). This catchment includes three fresh-water lakes (total area of 17 ha) that
112 are under regional protection since 1997 and are included in the European NATURA 2000
113 network as Site of Community Importance (SCI). The study area developed on Mesozoic and
114 Neogene materials that are composed by gypsiferous marls, dolimites, limestones, ophites and
115 sparse saline deposits. Karstic processes partially explain the evolution of the landscape of the
116 Estaña catchment with seventeen dolines (López-Vicente et al., 2009). Five of these dolines
117 reach the regional water table and explain the presence of lakes.

118 This area has a continental Mediterranean climate with two humid periods, one in spring
119 (April and May) and a second in autumn (September and October) and a dry summer with
120 frequent rainfall events of high intensity (López-Vicente et al., 2008). The average value of
121 annual precipitation is 619, 536 and 446 mm at the weather stations of Benabarre,
122 Camporrélls and Canelles, respectively, for the period 1997–2006 (Fig. 1). These weather
123 stations are located north-western, south-western, and south-eastern of the study area at a
124 distance of about 10 km. In spite of the short distance between the weather stations the
125 differences in the annual precipitation are explained by their geographical situation, between
126 the semiarid areas of the Ebro valley to the south and the humid areas of the Pyrenees to the
127 north.

128 The map of land use and land cover (*LULC*) of the study area presents sixteen different land
129 uses (Fig. 1) (López-Vicente, 2008) and shows the aspect of the typical Mediterranean agro-
130 ecosystem where natural and anthropogenic areas are heterogeneously distributed with
131 frequent changes in land uses from divides to slope-bottom and with a wide range of
132 extension from very small to large size polygons. Crops of winter barley is the main land use
133 (29% of the total surface) as well as dense (18%) and open (18%) Mediterranean forest and
134 dense (10%) and sparse (5%) scrublands whereas the other land uses occupies less than 5% of
135 the total surface and are spread around the study area. However, sparse scrublands are more

136 frequent in southern-orientated slopes (86% of total sparse scrublands) and oak forests are
 137 more frequent in northern orientated slopes (73% of total oak forests). Abandoned fields
 138 appear in steep slopes where many cropping terraces are tumbledown. Areas with outcrops of
 139 massive gypsum have been excluded in the study of soil erosion because the RUSLE model
 140 does not simulate erosion processes in rocks. Weather, land uses and tillage practices in the
 141 Estaña catchment are representative of rain-fed agricultural areas in Mediterranean
 142 mountainous agro-ecosystems.

143

144 **Estimation of Soil Loss: The RUSLE empirical model**

145 The RUSLE equation (Renard et al., 1997) predicts annual soil loss (A ; $\text{Mg ha}^{-1} \text{ yr}^{-1}$) as the
 146 product of the factors of rainfall and runoff erosivity (R ; $\text{MJ mm ha}^{-1} \text{ h}^{-1} \text{ yr}^{-1}$), soil erodibility
 147 (K ; $\text{Mg h MJ}^{-1} \text{ mm}^{-1}$), slope steep and length (LS , –), cover management (C , –) and support
 148 practices (P , –):

$$149 \quad A = R K L S C P \quad (1)$$

150

151 **Rainfall and runoff erosivity factor (R)**

152 The R factor assesses the effect of the rainfall impact on the soil surface as well as the
 153 magnitude of runoff and mathematically is defined as the sum of the storm erosivity index
 154 (EI_{30} ; $\text{MJ mm ha}^{-1} \text{ h}^{-1}$) of the total number of erosive storm events for the whole year
 155 according to the equations:

$$156 \quad R = \frac{1}{n} \sum_{j=1}^n \left[\sum_{k=1}^m (E)(I_{30})_k \right] \quad (2)$$

$$157 \quad EI_{30} = (E)(I_{30}) = \left(\sum_{K=1}^m e_r \Delta V_r \right) I_{30} \quad (3)$$

$$158 \quad e_r = 0.29[1 - 0.72 \exp(-0.05i_r)] \quad (4)$$

159 where E (MJ ha^{-1}) is the total storm energy, I_{30} (mm h^{-1}) is the maximum intensity in 30
 160 minutes, j is the number of erosive events for the n number of years, k is the temporal interval
 161 and m is the number of temporal intervals established for each storm event. The kinetic
 162 energy of a storm for each r period, e_r ($\text{MJ ha}^{-1} \text{ mm}^{-1}$), is estimated following the approach of
 163 Brown and Foster (1987) where ΔV_r (mm) is the volume of rainfall registered during the r
 164 period and i_r (mm h^{-1}) is the rainfall intensity for the r period. When $n = 1$ the calculated R
 165 value is the rainfall erosivity for one specific year.

166

167 **Soil erodibility factor (K)**

168 Soil erodibility is a complex property and is thought of as the ease with which the soil is
 169 detached by splash during rainfall or by runoff or both. The K factor is a lumped parameter
 170 that represents an integrated average annual value of the soil profile reaction to the processes
 171 of soil detachment and transport by raindrop impact and surface flow, localized deposition
 172 due to topography and tillage-induced roughness, and rainwater infiltration into the soil
 173 profile (Renard et al., 1997). This factor is assessed as a function of the soil organic content
 174 (SOC or OM , %), the product of the percentages of modified silt (2-100 μm) and sand (100-
 175 2000 μm) (M , -), classes of aggregates structure (s) and soil permeability (p):

$$176 \quad K = \frac{[2.1 \cdot 10^{-4} (12 - OM) M^{1.14} + 3.25 (s - 2) + 2.5 (p - 3)]}{100} 0.1317 \quad (5)$$

177 The RUSLE model established four different soil structure classes and six permeability
 178 classes (Table 1). The latest property can be estimated from the different classes of soil
 179 texture and from field estimation of the saturated hydraulic conductivity (K_{fs} , mm day^{-1}).

180 Surface rock fragments reduce significantly the splash detachment rates in a manner similar to
 181 the crop residues that protect the soil surface from raindrop impact. However, in coarse
 182 textured soils surface and subsurface rock fragments affect infiltration and thus runoff by
 183 reducing the soil void space and soil hydraulic conductivity and increasing the soil erodibility,
 184 especially in Mediterranean soils where stone pavements are frequent (Poesen et al., 1998)
 185 and significantly modified soil properties (Soto and Navas, 2004). In a previous study, López-
 186 Vicente et al. (2006a) observed an increase in the K factor in a set of old abandoned fields in
 187 the Estaña catchment due to the high content of coarse fragments in comparison with
 188 estimations without accounting the effect of rocks.

189 Although the percentage of coarse fragments varies along the soil in the same area, rocks
 190 appear in the soil profile as a frame, especially in interrill areas, where runoff cannot move
 191 them. Moreover, rock fragments larger than 2 mm were excluded when K values were
 192 estimated in Eq. (5). To account the effect of rocks in soil erodibility the RUSLE model
 193 includes the following approach:

$$194 \quad K_b / K_{fs} = (1 - R_w) \quad (6)$$

195 where K_b (mm day^{-1}) is the modified saturated hydraulic conductivity after accounting the
 196 effect of rock fragments, and R_w (%) is the weight percentage of coarse fragments. In this
 197 work, the soil erodibility factor is estimated from texture classification (K -texture) and
 198 infiltration measurements without (K - K_{fs}) and with (K - K_{fs} -rocks) corrections due to soil

199 stoniness. Finally, maps of the soil erodibility are equal to zero in urban areas and those with
 200 boulder grounds due to the absence of soil.

201

202 **Topographic factor (LS)**

203 The *LS* factor describes the combined effect of slope length and steepness and can be
 204 considered as a measurement of the sediment transport capacity by runoff. In this work, the
 205 *LS* factor has been calculated following the approach of Moore and Burch (Moore and
 206 Wilson, 1992) as a function of the net contributing area ($A_{s,i}$, m) and the slope angle (α_i ,
 207 radians). This approach is easy to run within a GIS application and has been satisfactorily
 208 used in other Mediterranean areas such as in northeast Spain (Martínez-Casasnovas and
 209 Sánchez-Bosch, 2000) and in south Italy (Di Stefano et al., 2000):

$$210 \quad LS_i = \left(\frac{A_{s,i}}{22.13} \right)^p \left(\frac{\sin \alpha_i}{0.0896} \right)^q \quad (7)$$

211 where p and q are two empirical exponents which values were assigned by Moore and Wilson
 212 (1992) as $p = 0.4$ and $q = 1.3$.

213

214 **Cover management factor (C)**

215 The *C* factor reflects the effect of cropping and management practices on erosion rates. The
 216 soil loss ratio (SLR_i) is an estimate of the ratio of soil loss under actual conditions to losses
 217 experienced under reference conditions (clean-tilled continuous-fallow). An individual SLR_i
 218 value is thus calculated for each time period i , as:

$$219 \quad SLR_i = PLU_i CC_i SR_i SC_i SM_i \quad (8)$$

220 where the sub-factors for each time period i are the prior land (PLU_i), the canopy cover (CC_i),
 221 the surface roughness (SR_i), the surface cover (SC_i), and the antecedent soil moisture (SM_i).
 222 Each SLR_i value is then weighted by the fraction of rainfall and runoff erosivity (EI_{30i} , %)
 223 associated with the corresponding time period, and these weighted values are combined into
 224 an overall *C* factor value as:

$$225 \quad C = \frac{1}{EI_{30t}} \sum_{i=1}^n EI_{30i} SLR_i \quad (9)$$

226 where EI_{30t} (%) is sum of EI_{30i} percentages for the entire time period, n is the total number of
 227 time periods i . The values of *C* factor ranges from 0 (total control of the erosion) to 1 (no
 228 effectiveness of cover-management practices). The equations for the sub-factors are the
 229 following:

$$230 \quad PLU_i = C_f C_b \exp\left[-\left(c_{ur} B_{ur}\right) + \left(c_{us} B_{us} / C_f^{c_{uf}}\right)\right] \quad (10)$$

$$231 \quad CC_i = 1 - F_c \exp(-0.1 H) \quad (11)$$

$$232 \quad SR_i = \exp[-0.66(R_u - 0.24)] \quad (12)$$

$$233 \quad SC_i = \exp\left[-b S_p \left(\frac{0.24}{R_u}\right)^{0.08}\right] \quad (13)$$

234 where C_f is a surface-soil-consolidation factor, C_b represents the relative effectiveness of
 235 subsurface residue in consolidation, B_{ur} (lb acre⁻¹ in⁻¹) is mass density of live and dead roots
 236 found in the upper inch of the soil, B_{us} is mass density of incorporated surface residue in the
 237 upper inch of the soil (lb acre⁻¹ in⁻¹), c_{uf} represents the impact of soil consolidation on the
 238 effectiveness of incorporated residue and c_{ur} and c_{us} are calibration coefficients indicating the
 239 impacts of subsurface residues. F_c (%) is fraction of land surface covered by canopy, H (ft) is
 240 distance that raindrops fall after striking the canopy, R_u (in) is surface roughness at initial
 241 conditions and just before tillage practices, b is an empirical coefficient that indicates the
 242 effectiveness of surface cover in reducing soil erosion and S_p (%) is percentage of land area
 243 covered by surface cover. Equations (10), (11), (12) and (13) were empirically formulated by
 244 using English units for their inputs. Antecedent soil moisture is an inherent component of
 245 continuous-tilled fallow plots, and these effects are reflected in the soil erodibility factor.
 246 Hence, no adjustment is made for changes in soil moisture to calculate the C factor.

247

248 ***Support practices factor (P)***

249 The P factor is the ratio of soil loss with a specific support practice on croplands to the
 250 corresponding loss with upslope and downslope tillage. Support practices in the study area
 251 include contouring (P_b sub-factor), stripcropping and buffer strips (P_b sub-factor) and
 252 terracing (P_t sub-factor). The P factor is calculated as the product of these sub-factors:

$$253 \quad P = P_b P_S P_t \quad (14)$$

254 The P_b sub-factor measures the effectiveness of orientated furrows and ridges determined by
 255 the tillage marks to modify the flow pattern, reducing the detachment and transport capacity
 256 by runoff. The P_S sub-factor describes how stripcropping and buffer strips, composed by grass
 257 and shrub species reduce soil erosion and trap sediments. The P_t sub-factor measures the
 258 effectiveness of terraces reducing sheet and rill erosion on the terrace interval by breaking the
 259 slope into shorter slope lengths. The P_t sub-factor is only effective in gentle areas with a slope
 260 value less than 0.9%. These sub-factors have been calculated from table values included in the

261 guide of the RUSLE model (Renard et al., 1997) according to the current tillage practices
262 (moldboard plow and cultivator), the map of land uses and after identifying and measuring the
263 length of the terraces in the study area.

264

265 **Validation with ^{137}Cs**

266 Application of ^{137}Cs technique has provided actual data of average net soil loss and deposition
267 for the last four decades. This technique has been applied in several areas as representative of
268 Mediterranean landscapes, such as in Spain (Navas, 1995; Quine et al., 1994) and Italy
269 (Stefano et al., 2005) and used as an excellent tool to test the accuracy of the spatially
270 distributed predictions of the RUSLE model (Hao et al., 2001). ^{137}Cs is an artificial
271 radionuclide that is strongly fixed to the fine fractions of the soil. Gamma emissions of ^{137}Cs
272 (in Bq kg^{-1} air-dry soil) were measured using a high resolution, low background, low energy,
273 coaxial gamma-ray detector of hyperpure germanium coupled to an amplifier and
274 multichannel analyser. Counting time was 30,000 s and the analytical precision of the
275 measurements was approximately $\pm 10\%$ (Navas et al., 2005). For this research, erosion rates
276 have been calculated by using fallout ^{137}Cs in eleven soil samples following the approach of
277 Soto and Navas (2004) adapted to Mediterranean soil conditions. The selected soil samples
278 are located in nine different fields of barley as representative of the different physiographic
279 conditions of the study area (Fig. 1).

280

281 **Database collection**

282 Rainfall erosivity has been calculated from values of precipitation at the weather station of
283 Canelles for the period 1997-2006 due to the higher temporal resolution of its record (each 15
284 minutes) in comparison with the weather stations of Camporrélls and Benabarre (daily
285 values). A total of 228 soil samples were collected in a regular net of 100 x 100 m (Fig. 1).
286 Samples were air-dried, ground, homogenized and quartered, to pass through a 2 mm sieve
287 and percentages of coarse fragments, clay, silt and sand and soil organic content (SOC) were
288 estimated. The corresponding maps of percentage of coarse fragments, silt, sand and organic
289 matter for the whole study area were obtained by spatial interpolation from data at sampling
290 points. Two types of structure of soil aggregate were identified for the different soil types
291 described at the study area by Machín et al. (2008) and the corresponding map was used to
292 calculate the sub-factor of soil structure. López-Vicente (2008) measured the saturated

293 hydraulic conductivity for each soil type obtaining values that range from 9.9 to 2252.5 mm
 294 day⁻¹ for Haplic Gypsisols and Haplic Leptosols, respectively.

295 The parameters of net contributing area and slope steepness of the *LS* factor have been
 296 calculated from the enhanced digital elevation model of the Estaña catchment (López-Vicente
 297 et al., 2009) and using a combined flow accumulation algorithm that has proven to better
 298 describe the spatial distribution of accumulated surface flow in comparison with simple and
 299 multiple flow algorithms (López-Vicente et al., 2006b). In this work, the threshold value of
 300 the combined algorithm has been associated to the beginning of the gullies to obtain a more
 301 accurate description of the hydrological processes.

302 The *C* factor for barley fields was calculated from the *SLR* values for periods of fifteen days
 303 estimated by López-Vicente et al. (2008) for a selected set of fields in the study area whereas
 304 an annual constant value of *C* was calculated for the other land uses from table values
 305 included in the guide of the RUSLE model (Renard et al., 1997) and in Table 2. In this work,
 306 the parameter of rainfall interception by canopy (*I*, 0 – 1) has been added for a better
 307 assessment of the canopy cover sub-factor following the approach of Morgan (2001) and
 308 values included in Table 2. Rainfall interception is defined as the amount of rainfall that
 309 remains in the branches and leaves of the canopy and crop residues and returns to the
 310 atmosphere by evaporation.

311

312 **RESULTS AND DISCUSSION**

313 Values of rainfall erosivity and maximum intensity range between 2 and 1216.3 MJ mm ha⁻¹
 314 h⁻¹ and between 1.6 and 69.8 mm h⁻¹, respectively, with mean values of 81.3 MJ mm ha⁻¹ h⁻¹
 315 and 15.2 mm h⁻¹. The mean value of the *R* factor is 1000.3 MJ mm ha⁻¹ h⁻¹ yr⁻¹, with a
 316 minimum of 215 MJ mm ha⁻¹ h⁻¹ yr⁻¹ in 2004 and a maximum of 1969.2 MJ mm ha⁻¹ h⁻¹ yr⁻¹
 317 in 1998. The three estimated maps of soil erodibility present similar mean values that range
 318 between 0.009 and 0.011 Mg h MJ⁻¹ mm⁻¹ for *K-K_{fs}* and *K-texture*, respectively, though
 319 maximum values and areas with low values vary significantly between *K-texture* and the
 320 other two approaches (Fig. 2). The maximum value of soil erodibility is equal for *K-K_{fs}* and
 321 *K-K_{fs}-rocks* and is 39% higher than that obtained with *K-texture*. In the three maps those areas
 322 associated to soil samples with loam and sandy loam textures and blocky and massive
 323 structure present high values of soil erodibility whereas soils with silty clay loam texture and
 324 medium or coarse granular structure present low values. Soil erodibility maps calculated from
 325 infiltration values present a higher spatial variability and complexity that is related to the
 326 different soil types. Coarse fragments reduce the saturated hydraulic conductivity in a

327 percentage of 30.7% that is similar to the mean percentage of coarse fragments in the soil
 328 profile for the study area. However, the effect of these changes in the values of the class
 329 permeability sub-factor of the Eq. (5) is limited to those areas with high values of coarse
 330 fragments obtaining a mean value of $K-K_{fs-rocks}$ that is only 6.1% higher than the value
 331 calculated for $K-K_{fs}$. Maps of $K-K_{fs}$ and $K-K_{fs-rocks}$ present a value of zero in areas with high
 332 values of soil organic content (SOC), saturated hydraulic conductivity and percentage of
 333 coarse fragments.

334 The map of the LS factor has a mean value of 5.1 and a maximum of 61.3 (Fig. 2.d). Steep
 335 areas and those located in gullies present high values of the LS factor, whereas flat areas
 336 ($\alpha_i = 0$) that represent a percentage of 0.14% of the study area, have a value of zero. The LS
 337 factor presents low values at headwater due to the key role of the map of flow accumulation
 338 in these areas, whereas in the rest of the flow-path the LS factor is more sensitive to the
 339 parameter of slope steepness. The map of the C factor has a mean value of 0.072 and is very
 340 sensitive to the different land uses (Fig. 2.e). The highest values (low soil protection) are
 341 associated to paths and crops and the lowest (high soil protection) to dense scrublands,
 342 poplars, pine woodlands and pastures.

343 The map of P factor has a mean value of 0.76 and minimum of 0.6 in barley fields and 1.0 in
 344 the rest of the study area (Fig. 2.f). Stripcropping is the most effective support practice and
 345 explain the lowest values of the P factor in the steep small fields of the study area. Contouring
 346 effectiveness is sensitive to slope steepness being non-effective in a percentage of 2.4% of the
 347 area of the fields and explains the values of the P factor of the fields that surround the lakes.
 348 From a total of 32 terraced fields in the study area (4.2 ha) the P_t sub-factor only reduces the
 349 predicted rates of soil loss in three pixels (75 m^2) with values of 0.55, 0.69 and 0.8 and a
 350 mean value for the total surface of barley fields of 0.9994.

351 Potential annual soil loss (A_p , $\text{Mg ha}^{-1} \text{ yr}^{-1}$) is estimated from the product of the R , K and LS
 352 factors and represents the scenario of a total lack of vegetation and support practices. Potential
 353 and actual maps of soil loss are calculated with the more complex approach of the $K-K_{fs-rocks}$
 354 factor. The mean value of A_p for the Estaña catchment is $54.1 \text{ Mg ha}^{-1} \text{ yr}^{-1}$ being lower than
 355 the mean value of $95.1 \text{ Mg ha}^{-1} \text{ yr}^{-1}$ calculated by Onori et al. (2006) in the Comunelli
 356 catchment (Sicily, Italy) with the RUSLE model and similar to that of $55.4 \text{ Mg ha}^{-1} \text{ yr}^{-1}$
 357 estimated by Sadiki et al. (2004) in the Rif mountains of Morocco with the USLE model. The
 358 average soil erosion rate estimated with the RUSLE model for the study area is 2.3 Mg ha^{-1}

359 yr⁻¹ (Fig. 3). This lower rate by comparing with the potential erosion highlights the key role of
360 vegetation cover and conservation practices in reducing soil erosion rates.

361 Tolerable soil loss (T ; Mg ha⁻¹ yr⁻¹) is defined as the maximum rate of soil erosion that can
362 occur and still permit crop productivity to be sustained economically after considering rates of
363 soil formation. Values of T range from 2.2 to 11.2 Mg ha⁻¹ yr⁻¹ according to the RUSLE
364 model for soils in the USA. In Spain, De la Horra (1992) calculated a mean value of T of 6
365 Mg ha⁻¹ yr⁻¹ at the province of Toledo (Central Spain) that was used by Boellstorff and Benito
366 (2005) to compare the estimated rates of soil erosion with RUSLE in the same area and used
367 in this work to evaluate the predicted rates of soil loss. A maximum of 40 Mg ha⁻¹ yr⁻¹ is
368 considered as the limit between very high and irreversible stages of soil loss. The histogram
369 of the map of predicted soil loss shows that 88% of the soil surface at the Estaña catchment
370 has low and medium rates of erosion and only 1.8% of the surface high, very high and
371 irreversible rates (Fig. 3). Flat areas and those which K factor value is zero present no erosion
372 and only represent 0.4% of the total study area.

373 Validation with ¹³⁷Cs of estimated soil erosion in barley fields with RUSLE with the three
374 different approaches for estimating the K factor shows that estimation of soil losses with the
375 K - K_{fs} -*rocks* factor lightly improves the model predictions in comparison with the predictions
376 obtained with the K -*texture* and K - K_{fs} factors (Table 3). The estimated rates of soil erosion
377 with the three different approaches are lower than the measured rate with ¹³⁷Cs. This situation
378 can be explained by the low values of precipitation recorded at the Canelles weather station
379 during the period 1997–2006 (mean annual precipitation of 446 mm) in comparison with the
380 mean annual precipitation during the last four decades (mean annual precipitation during the
381 reference period of 1961–1990 of 520 mm). Furthermore, it is necessary to consider that
382 predicted values are modelled for a raster cell area of 5 x 5 meters whereas control points are
383 representative of punctual measurements.

384 Trails present the highest average value of soil loss (19 Mg ha⁻¹ yr⁻¹) that is explained by the
385 high value of the C factor (Table 4). Total erosion for this land use represents 14% of the total
386 erosion predicted for the Estaña catchment though its total surface is only 2% of the total area.
387 Therefore, paths and trails are small-scale anthropogenic disturbances that strongly contribute
388 to soil degradation. These results agree with those obtained by several authors in other areas
389 in the world (e.g. Ricker et al., 2008; Rijdsdijk et al., 2007).

390 The mean value of erosion for barley fields in steep areas is 5.8 Mg ha⁻¹ yr⁻¹ that is almost
391 equal to the tolerable value of erosion proposed by De la Horra (1992). Total soil loss in these
392 fields represents 44% of total erosion in the Estaña catchment and only 18% of the surface of

393 the study area. Furthermore, the average value of soil loss in steep fields is 56% higher than
394 the average rate estimated for fields in gentle areas. These land uses with tolerable and very
395 high rates of erosion also have areas with very low rates, even no erosion.

396 Open Mediterranean forest, barley fields in gentle areas and disperse scrubland present low
397 average values ($1 - 4 \text{ Mg ha}^{-1} \text{ yr}^{-1}$) of soil erosion whereas the rest of land uses has very low
398 rates of soil loss (less than $1 \text{ Mg ha}^{-1} \text{ yr}^{-1}$) (Table 4). The average soil erosion rate for the
399 areas with anthropogenic land uses ($4.21 \text{ Mg ha}^{-1} \text{ yr}^{-1}$) is 4.4 times higher than that estimated
400 for the areas with natural vegetation ($0.96 \text{ Mg ha}^{-1} \text{ yr}^{-1}$). These results agree with those
401 calculated by Sadiki et al. (2007) with ^{137}Cs in Morocco where cereal crops have average
402 values of soil loss much higher than those on scrubland and fallow land.

403 Within the areas of natural vegetation, the average value of soil erosion in scrublands is lower
404 than the average value in Mediterranean forest. These results agree with those obtained by
405 Casermeiro et al. (2004) in Central Spain and by Navas and Walling (1992) in north-eastern
406 Spain and highlight the more effective role of shrubs to avoid soil erosion and promote
407 sediment accumulation. In areas of anthropogenic land uses there is a decrease in the
408 estimated value of soil loss in relation to the age of abandonment of fields (Table 4) and an
409 increase in the percentage of soil organic content (SOC) from 2.7 to 3.9% and of coarse
410 fragments from 23 to 36%. These results are associated to complex processes of natural
411 vegetation re-growth and exportation of fine particles of the soil profile, especially in top soil
412 layers. Values of soil loss, SOC and percentage of coarse fragments in old abandoned fields
413 are almost equal to those obtained in dense Mediterranean forest. Hence, soil quality in old
414 abandoned fields has achieved the standards of natural soils in the Estaña catchment. These
415 results disagree with those calculated by Navas et al. (1997) in Central Pyrenees where
416 abandoned fields have higher values of soil loss than those in fields in use and highlight the
417 complexity and spatial heterogeneity of the processes of soil erosion and recovery in
418 Mediterranean abandoned farmlands.

419 Cultivated soils present higher rates of soil erosion than those soils in scrublands and oak and
420 Mediterranean forest for the different parent materials and slope steepness conditions in the
421 study area (Fig. 4). Cultivated soils developed over clay materials in high slope areas present
422 the highest soil erosion rates and are the most susceptible to suffer intense soil erosion (higher
423 than $8 \text{ Mg ha}^{-1} \text{ yr}^{-1}$). Soils developed over limestones in forested areas with low and medium
424 slope present the lowest values of soil erosion (less than $1 \text{ Mg ha}^{-1} \text{ yr}^{-1}$).

425 Statistical analysis of each factor at sampling points shows that the cover-management factor
426 (C) contributes most of the variability of the values of predicted soil erosion, the *K* and *LS*

427 factors contribute a similar amount and the *P* factor contributes least to the variability of *A*.
428 The *R* factor is not considered in the analysis because of its constant value for the study area.
429 The high number of inputs to calculate the *C* factor and of land uses in Mediterranean
430 landscapes suggests the necessity of field measurements of these parameters, especially in
431 areas with natural vegetation where the *C* factor has very low values. On the other hand, the
432 addition of an antecedent soil moisture sub-factor to the soil erodibility factor may improve its
433 quality predictions due to the seasonal variability of this soil property in Mediterranean
434 environments (López-Vicente et al., 2008) and its importance in soil saturation and runoff
435 processes (Terzoudi et al., 2007). To promote sustainable strategies we propose to delay the
436 plowing practices just before seeding to extend the protection role by the crop residues
437 accounted in the *C* factor. We also propose to recover tumbledown cropping terraces that
438 appear in the steep slopes of the study area to increase the effect of the *P* factor to reduce the
439 magnitude of overland flow and to increase the trap efficiency of soil eroded particles by
440 vegetation. These practices can be applied in other Mediterranean agro-ecosystems to avoid
441 soil erosion and thus to promote sustainable agricultural practices.

442

443 CONCLUSIONS

444 The application of the RUSLE model with a high resolution database of its input values
445 allows detailed mapping of spatially distributed soil erosion rates at the Estaña catchment.
446 The more complex approach of the *K* soil erodibility factor calculated from field infiltration
447 measurements and accounting the effect of coarse fragments improves estimations of soil
448 erosion rates in barley fields and fits best with the quantified values of soil loss with ¹³⁷Cs.
449 Hence, the consideration of these soil properties is of interest for a better application of the
450 RUSLE model in Mediterranean environments where stone pavements are frequent and
451 modify the saturated hydraulic conductivity of the soil.

452 Although soil erosion does not appear to be a problem for most of the study area high and
453 very high values of soil loss are estimated for crops in steep areas and developed over clay
454 materials. The average value of soil loss in areas with human disturbances (cultivated and
455 abandoned fields and paths) is more than four times higher than that estimated for areas with
456 natural vegetation. The RUSLE model predicts a decrease in the values of soil erosion in
457 fields in accordance with the increase of the age of abandonment. Predicted values of soil
458 erosion and measured of soil organic content (SOC) and stoniness in old abandoned fields are
459 comparable with those in areas of natural forest and suggest a recovery of the original soil
460 conditions.

461 The *C* factor explains most of the variability of the predicted values of soil erosion and its
462 more detailed estimation may be done in forthcoming research to improve quality predictions
463 of soil loss. Conservation policies should be established in areas with clay materials in steep
464 cultivated and not cultivated slopes to avoid an irreversible state of soil degradation. The
465 delay of plowing practices and the recovery of tumbledown cropping terraces are suggested as
466 sustainable agricultural practices to reduce soil erosion in Mediterranean agro-ecosystems.

467

468 **ACKNOWLEDGEMENTS**

469 *This research was financially supported by the following project: “Soil erosion and carbon*
470 *dynamic in Mediterranean agroecosystems: radioisotopic modelling at different spatial and*
471 *temporal scales” (MEDEROCAR, CGL2008-00831/BTE) funded by the Spanish Ministry of*
472 *Science and Innovation.*

473

474 **REFERENCES**

- 475 Alpert, P., Ben-Gai, T., Baharad, A., Benjamín, Y., Yekutieli, D., Colación, M., Diodato, L., Ramis,
476 C., Homar, V., Romero, R., Michaelides, S., and A. Manes. 2002. The paradoxical increase of
477 Mediterranean extreme daily rainfall in spite of decrease in total values. *Geophys. Res. Lett.*
478 29(11): 1536.
- 479 Arhonditsis, G., Giourga, C., Loumou, A., and M. Koulouri. 2002. Quantitative assessment of
480 agricultural runoff and soil erosion using mathematical modeling: Applications in the
481 Mediterranean region. *Environ. Manage.* 30: 434–453.
- 482 Ashby, M. 1999. Modelling the water and energy balances of Amazonian rainforest and pasture using
483 Anglo-Brazilian Amazonian climate observation study area. *Agr. Forest Meteorol.* 94: 79–101.
- 484 Bartsch, K.P., Van Miegroet, H., Boettinger, J., and J. P. Dobrowolski. 2002. Using empirical erosion
485 models and GIS to determine erosion risk at Camp Williams, Utah. *J. Soil Water Conserv.* 57(1):
486 29–37.
- 487 Belmonte, F., and A. Romero. 1998. La cubierta vegetal en las regiones áridas y semiáridas:
488 consecuencias de la interceptación de la lluvia en la protección del suelo y los recursos hídricos /
489 Canopy cover in arid and semi-arid regions: consequences of rainfall interception on soil protection
490 and water resources. *NORBA-Journal of Geography* 10: 9–22.
- 491 Boellstorff, D., and G. Benito. 2005. Impacts of set-aside policy on the risk of soil erosion in central
492 Spain. *Agr. Ecosyst. Environ.* 107: 231–243.
- 493 Brown, L.C., and G. R. Foster. 1987. Storm erosivity using idealized intensity distributions, T. *ASAE*
494 30: 379–386.

- 495 Carreiras, J.M.B., Pereira, J.M.C., and J. S. Pereira. 2006. Estimation of tree canopy cover in
496 evergreen oak woodlands using remote sensing. *Forest Ecol. Manag.* 223: 45–53.
- 497 Casermeiro, M.A., Molina, J.A., de la Cruz Caravaca, M.T., Hernando Costa, J., Hernando Massanet,
498 M.I., and P. S. Moreno. 2004. Influence of scrubs on runoff and sediment loss in soils of
499 Mediterranean climate. *Catena* 57: 91–107.
- 500 COM (Commission of the European Communities). 2006. Proposal for a Directive of the European
501 Parliament and of the Council establishing a framework for the protection of soil and amending
502 Directive 2004/35/EC (presented by the Commission). COM(2006) 232 final. 2006/0086 (COD).
503 Brussels, Belgium.
- 504 Corbane, C., Andrieux, P., Voltz, M., Chadœuf, J., Albergel, J., Robbez-Masson, J.M., and P. Zante.
505 2008. Assessing the variability of soil surface characteristics in row-cropped fields: The case of
506 Mediterranean vineyards in Southern France. *Catena* 72(1): 79–90.
- 507 De la Horra, J.L. 1992. Aspectos biogeográficos en relación con la problemática agraria de la comarca
508 de Torrijos (Toledo) / Biogeographic aspects in relation with the problematic agricultura in
509 Torrijos. Ph.D. Thesis, Universidad Complutense de Madrid, Spain.
- 510 de Paz, J.-M., Sánchez, J., and F. Visconti. 2006. Combined use of GIS and environmental indicators
511 for assessment of chemical, physical and biological soil degradation in a Spanish Mediterranean
512 region. *J. Environ. Manage.* 79(2): 150–162.
- 513 Desir, G., and C. Marín. 2007. Factors controlling the erosion rates in a semi-arid zone (Bardenas
514 Reales, NE Spain). *Catena* 71(1): 31–40.
- 515 Di Stefano, C., Ferro, V., and P. Porto. 2000. Length Slope Factors for applying the Revised Universal
516 Soil Loss Equation at Basin Scale in Southern Italy. *J. Agr. Eng. Res.* 75: 349–364.
- 517 Eberbach, P., and M. Pala. 2005. Crop row spacing and its influence on the partitioning of
518 evapotranspiration by winter-grown wheat in Northern Syria. *Plant Soil* 268: 195–208.
- 519 EPC (European Parliament and of the Council). 2004. Directive 2004/35/CE of the European
520 Parliament and of the Council of 21 April 2004 on environmental liability with regard to the
521 prevention and remedying of environmental damage. *Official Journal of the European Union L*
522 143/56.
- 523 Hammad, A.A., Lundekvam, H., and T. Børresen. 2004. Adaptation of RUSLE in the Eastern Part of
524 the Mediterranean Region. *Environ. Manage.* 34(6): 829–841.
- 525 Hao, Y., Lal, R., Izaurralde, R.C., Ritchie J.C., Owens, L.B., and D. L. Hothem. 2001. Historic
526 assessment of agricultural impacts on soil and soil organic carbon erosion in an Ohio watershed.
527 *Soil Sci.* 166(2): 116–126.
- 528 IISD. 2007. Summary of the first extraordinary session of the conference of the parties to the UNCCD:
529 26 november 2007. *Earth Negotiations Bulletin* 4(207): 1–2.
- 530 IPE-GA. 2005. Atlas de la Flora de Aragón/Atlas of the vegetation of Aragon. Available from:
531 <http://www.ipe.csic.es/floragon/>. © Copyright 2005

- 532 Jetten, V., Govers, G., and R. Hessel. 2003. Erosion models: Quality of spatial predictions. *Hidrol.*
533 *Process.* 17(5): 887–900.
- 534 Kéfi, S., Rietkerk, M., Alados, C.L., Pueyo, Y., Papanastasis, V.P., ElAich, A., and P. C. de Ruiter.
535 2007. Spatial vegetation patterns and imminent desertification in Mediterranean arid ecosystems.
536 *Nature* 449(7159): 213–217.
- 537 Lewis, L.A., Verstraeten, G., and H. L. Zhu. 2005. RUSLE applied in a GIS framework: Calculating
538 the LS factor and deriving homogeneous patches for estimating soil loss. *Int. J. Geogr. Inf. Sci.*
539 19(7): 809–829.
- 540 Llorens, P., and F. Domingo. 2007. Rainfall partitioning by vegetation under Mediterranean
541 conditions. A review of studies in Europe. *J. Hydrol.* 335: 37–54.
- 542 López-Bermúdez, F. 1990. Soil erosion by water on the desertification of a semi-arid Mediterranean
543 fluvial basin: the Segura basin, Spain. *Agr. Ecosyst. Environ.* 33(2): 129–145.
- 544 López-Vicente, M. 2008. Erosión y redistribución del suelo en agroecosistemas mediterráneos:
545 Modelización predictiva mediante SIG y validación con ¹³⁷Cs (Cuenca de Estaña, Pirineo Central) /
546 Soil erosion and redistribution in Mediterranean agro-ecosystems: predictive modelling with GIS
547 and validation with ¹³⁷Cs (Estaña catchment, Spanish Central Pyrenees). University of Zaragoza,
548 Spain.
- 549 López-Vicente, M., A. Navas, and J. Machín. 2006a. Variation of soil erodibility in abandoned fields:
550 A case study in the Carrodilla Range (Spanish Pyrenees). In *Soil and Water Conservation Under*
551 *Changing Land Use*. Martínez-Casasnovas J.A., I. Pla Sentís, M.C. Ramos Martín, J.C. Balasch
552 Solanes (eds.). Universitat de Lleida. Lérida, Spain. pp. 167-170.
- 553 López-Vicente, M., Navas, A., and J. Machín. 2008. Identifying erosive periods by using RUSLE
554 factors in mountain fields of the Central Spanish Pyrenees. *Hydrol. Earth Syst. Sc.* 12(2): 1–13.
- 555 López-Vicente, M., A. Navas, and J. Machín. 2009. Geomorphic mapping in endorheic subcatchments
556 in the Spanish Pyrenees: An integrated GIS analysis of topographic-karstic features.
557 *Geomorphology* DOI: 10.1016/j.geomorph.2008.03.014.
- 558 López-Vicente, M., Navas, A., Machín, J., and L. Gaspar. 2006b. Modelización de la pérdida de suelo
559 en una cuenca endorreica del Pirineo oscense / Modelling soil loss in an endorheic catchment of the
560 Spanish Pyrenees. *Cuadernos de Investigación Geográfica* 32: 29–42.
- 561 Lufafa, A., Tenywa, M.M., Isabirye, M., Majaliwa, M.J.G., and P. L. Woomer. 2003. Prediction of
562 soil erosion in a Lake Victoria basin catchment using a GIS-based Universal Soil Loss model. *Agr.*
563 *Syst.* 76(3): 883–894.
- 564 Machín, J., López-Vicente, M., and A. Navas. 2008. Cartografía digital de suelos de la Cuenca de
565 Estaña (Prepirineo Central) / Digital mapping of soils of the Estaña catchment (Central Pre-
566 Pyrenees). In: Benavente, J., and F. J. Gracia (Eds.): *Trabajos de Geomorfología en España, 2006-*
567 *2008*. SEG. Cádiz, Spain, pp. 477-480.

- 568 Martínez-Casasnovas, J.A., and I. Sánchez-Bosch. 2000. Impact assessment of changes in land
569 use/conservation practices on soil erosion in the Penedès–Anoia vineyard region (NE Spain). *Soil*
570 *Till. Res.* 57: 101–106.
- 571 Moore, I.D., and J. P. Wilson. 1992. Length-slope factors for the Revised Universal Soil Loss
572 Equation: simplified method of estimation. *J. Soil Water Conserv.* 47(5): 423–428.
- 573 Morschel, J., Fox, D.M., and J.-F. Bruno. 2004. Limiting sediment deposition on roadways:
574 topographic controls on vulnerable roads and cost analysis of planting grass buffer strips. *Environ.*
575 *Sci. Policy* 7: 39–45.
- 576 Morgan, R.P.C. 2001. A simple approach to soil loss prediction: a revised Morgan–Morgan–Finney
577 model. *Catena* 44: 305–322.
- 578 Nagler, P.L., Glenn, E.P., Thompsona, T.L., and A. Huete. 2004. Leaf area index and normalized
579 difference vegetation index as predictors of canopy characteristics and light interception by riparian
580 species on the Lower Colorado River. *Agr. Forest Meteorol.* 125: 1–17.
- 581 Navas, A. 1995. Cuantificación de la erosión mediante el radioisótopo cesio 137. *Sociedad Española*
582 *de Geomorfología / Assessment of erosion with the radioisotop Caesium 137. Cuadernos Técnicos*
583 *de la SEG*, 8.
- 584 Navas, A., García-Ruiz, J.M., Machín, J., Lasanta, T., Walling, D., Quine, T., and B. Valero. 1997.
585 Aspects of soil erosion in dry farming land in two changing environments of the central Ebro
586 valley, Spain. *IAHS Publi.* 245: 13–20.
- 587 Navas, A., Machín, J., and J. Soto. 2005. Assessing soil erosion in a Pyrenean mountain catchment
588 using GIS and fallout ¹³⁷Cs. *Agr. Ecosyst. Environ.* 105(3): 493–506.
- 589 Navas, A., and D. Walling. 1992. Using caesium-137 to assess sediment movement in a semiarid
590 upland environment in Spain. *IAHS* 209: 129–138.
- 591 Navas, A., Walling, D.E., Quine, T., Machín, J., Soto, J., Domenech, S., and M. López-Vicente. 2007.
592 Variability in ¹³⁷Cs inventories and potential climatic and lithological controls in the central Ebro
593 valley, Spain. *J. Radioanal. Nucl. Ch.* 274(2): 331–339.
- 594 Nisar Ahamed, T.R., Gopal Rao, K., and J. S. R. Murthy. 2000. Fuzzy class membership approach to
595 soil erosion modelling. *Agr. Syst.* 63(2): 97–110.
- 596 Onori, F., De Bonis, P., and S. Grauso. 2006. Soil erosion prediction at the basin scale using the
597 revised universal soil loss equation (RUSLE) in a catchment of Sicily (southern Italy). *Environ.*
598 *Geol.* 50: 1129–1140.
- 599 Pelacani, S., Märker, M., and G. Rodolfi. 2008. Simulation of soil erosion and deposition in a
600 changing land use: A modelling approach to implement the support practice factor.
601 *Geomorphology* 99(1-4): 329–340.
- 602 Poesen, J.W., van Wesemael, B., Bunte, K., and A. Solé-Benet. 1998. Variation of rock fragment
603 cover and size along semiarid hillslopes: a case-study from southeast Spain. *Geomorphology* 23:
604 323–335.

- 605 Quine, T., Navas, A., Walling, D.E., and J. Machín. 1994. Soil erosion and redistribution on cultivated
606 and uncultivated land near Las Bardenas in the Central Ebro River Basin, Spain. *Land Degrad.*
607 *Rehabil.* 5: 41–55.
- 608 Rambal, S., Ourcival, J.M., Offre, R.J., Mouillot, F., Nouvellon, Y., Reichstein, M., and A. Rocheteau.
609 2003. Drought controls over conductance and assimilation of a Mediterranean evergreen
610 ecosystem: scaling from leaf to canopy. *Global Change Biol.* 9: 1813–1824.
- 611 Renard, K.G., Foster, G.R., Weesies, G.A., McCool, D.K., and D. C. Yoder. 1997. Predicting Soil
612 Erosion by Water: A Guide to Conservation Planning with the Revised Universal Soil Loss
613 Equation (RUSLE). Handbook #703. US Department of Agriculture, Washington, DC.
- 614 Renard, K.G., Foster, G.R., Weesies, G.A., and J. P. Porter. 1991. RUSLE – Revised universal soil
615 loss equation. *J. Soil Water Conserv.* 46(1): 30–33.
- 616 Ricker, M.C., Odhiambo, B.K., and J. M. Church. 2008. Spatial analysis of soil erosion and sediment
617 fluxes: A paired watershed study of two Tappahannock River tributaries, Stafford County,
618 Virginia. *Environ. Manage.* 41(5): 766–778.
- 619 Rijdsdijk, A., Sampurno Bruijnzeel, L.A., and C. Kukuh Sutoto. 2007. Runoff and sediment yield from
620 rural roads, trails and settlements in the upper Konto catchment, East Java, Indonesia.
621 *Geomorphology* 87: 28–37.
- 622 Rodríguez, A.B.M., and S. Schnabel. 1998. Medición de la interceptación de las precipitaciones por la
623 encina (*Quercus rotundifolia* lam.): metodología e instrumentalización / Measurement of rainfall
624 interception by oak trees (*Quercus rotundifolia* lam.): methodology and instrumentation. *NORBA-*
625 *Journal of Geography* 10: 95–112.
- 626 Rodríguez-Calcerrada, J., Pardos, J.A., Gil, L., and I. Aranda. 2007. Summer field performance of
627 *Quercus petraea* (Matt.) Liebl and *Quercus pyrenaica* Willd seedlings, planted in three sites with
628 contrasting canopy cover. *New Forest.* 33: 67–80.
- 629 Sadiki, A., Bouhlassa, S., Auajjar, J., Faleh, A., and J. J. Macaire. 2004. Utilisation d'un SIG pour
630 l'évaluation et la cartographie des risques d'érosion par l'Equation universelle des pertes en sol
631 dans le Rif oriental (Maroc): cas du bassin versant de l'oued Boussouab. *Bulletin de l'Institut*
632 *Scientifique, Rabat, section Sciences de la Terre* 26: 69–79.
- 633 Sadiki, A., Faleh, A., Navas, A., and S. Bouhlassa. 2007. Assessing soil erosion and control factors by
634 the radiometric technique in the Boussouab catchment, Eastern Rif, Morocco. *Catena* 71(1): 13–20.
- 635 Soto, J., and A. Navas. 2004. A model of ¹³⁷Cs activity profile for soil erosion studies in uncultivated
636 soils of Mediterranean environments. *J. Arid Environ.* 59: 719–730.
- 637 Spaeth Jr., K.E., Pierson Jr., F.B., Weltz, M.A., and W. H. Blackburn. 2003. Evaluation of USLE and
638 RUSLE estimated soil loss on rangeland. *J. Range Manage.* 56(3): 234–246.
- 639 Staelens, J., De Schrijver, A., Verheyen, K., and N. E. C. Verhoest. 2006. Spatial variability and
640 temporal stability of throughfall water under a dominant beech (*Fagus sylvatica* L.) tree in
641 relationship to canopy cover. *J. Hydrol.* 330: 651– 662.

- 642 Stefano, C.D., Ferro, V., Porto, P., and S. Rizzo. 2005. Testing a spatially distributed sediment
643 delivery model (SEDD) in a forested basin by cesium-137 technique. *J. Soil Water Conserv.* 60(3):
644 148–157.
- 645 Tapiador, F.J., Sanchez, E., and M. A. Gaertner. 2007. Regional changes in precipitation in Europe
646 under an increased greenhouse emissions scenario. *Geophys. Res. Lett.* 34(6): L06701.
- 647 Tejada, M., and J. L. Gonzalez. 2006. The relationships between erodibility and erosion in a soil
648 treated with two organic amendments. *Soil Till. Res.* 91: 186–198.
- 649 Terzoudi, C.B., Gemtos, T.A., Danalatos, N.G., and I. Argyrokastritis. 2007. Applicability of an
650 empirical runoff estimation method in central Greece. *Soil Till. Res.* 92: 198–212.
- 651 Thornes, J.B. 2007. Modelling Soil Erosion by Grazing: Recent Developments and New Approaches.
652 *Geogr. Res.* 45(1): 13–26.
- 653 Vicente-Serrano, S.M., and J. M. Cuadrat-Prats. 2007. Trends in drought intensity and variability in
654 the middle Ebro valley (NE of the Iberian peninsula) during the second half of the twentieth
655 century. *Theor. Appl. Climatol.* 88(3–4): 247–258.
- 656 Zuazo, V.H.D., Martínez, J.R.F., and A. M. Raya. 2004. Impact of vegetative cover on runoff and soil
657 erosion at hillslope scale in Lanjaron, Spain. *Environmentalist* 24(1): 39–48.
- 658
- 659

660 **TABLE 1.** Classes of soil permeability and structure according to the different types of texture, infiltration
 661 properties and type of aggregates.

Permeability class	Texture	Saturated hydraulic conductivity
		(mm h ⁻¹)
1	Sand	> 61.0
2	Loamy sand, sandy loam	20.3 – 61.0
3	Loam, silt loam	5.1 – 20.3
4	Sandy clay loam, clay loam	2.0 – 5.1
5	Silty clay loam, sand clay	1.0 – 2.0
6	Silty clay, clay	< 1.0
Structure class	Type of soil aggregate structure	
1	Very fine granular (< 1 mm)	
2	Fine granular (1 – 2 mm)	
3	Medium or coarse granular (2 – 10 mm)	
4	Blocky, platy or massive (> 10 mm)	

662

663 **TABLE 2.** Summary of values for calculating the cover management factor for the different land-uses.

Land-use and land-cover type		PH (m)	CC (%)	RI (%)
Anthropogenic	Path	0	0	0
Use	Winter barley	0-0.46 ⁽¹⁾ ; 0.10*	30.42 ⁽¹⁾	0-3 ^{**} (2) -14 ⁽³⁾ ; 7.33*
	Pasture	0.28 ⁽²⁾	100 ⁽¹⁾	8.33 ⁽²⁾
	Olive and almond trees	10 ⁽⁴⁾	27.5 ⁽⁵⁾	23.67 ⁽⁶⁾
	Old abandoned fields	5.5 ⁽⁴⁾	80.7 ⁽⁷⁾	22.5 ⁽⁸⁾
	Recent abandoned fields	1 ⁽⁴⁾	27.5 ⁽⁵⁾	30.8 ⁽⁹⁾
Natural vegetation	Oak forest	20 ⁽⁴⁾	80.7 ⁽⁷⁾	23.67 ⁽⁶⁾
	Dense Mediterranean forest	5.5 ⁽¹⁰⁾	80.7 ⁽⁷⁾	22.5 ⁽⁸⁾
	Open Mediterranean forest	2 ⁽⁴⁾	27.5 ⁽⁵⁾	22.5 ⁽⁸⁾
	Dense scrubland	1 ⁽¹⁰⁾	80.7 ⁽⁷⁾	30.8 ⁽⁹⁾
	Disperse scrubland	1 ⁽¹⁰⁾	27.5 ⁽⁵⁾	30.8 ⁽⁹⁾
	Poplar	25 ⁽⁴⁾	98 ⁽¹¹⁾	23.67 ⁽⁶⁾
	Bank vegetation	3 ⁽⁴⁾	100 ⁽¹⁾	8.33 ⁽²⁾
	Pine woodland	10 ⁽¹²⁾	80.7 ⁽⁷⁾	24 ⁽¹²⁾

664 PH: Plant height. CC: Canopy cover. RI: Rainfall interception. * Average annual value. ** Crop residues. ⁽¹⁾Renard
665 et al. (1997); ⁽²⁾Ashby (1999); ⁽³⁾Eberbach and Pala (2005); ⁽⁴⁾IPE-GA (2005); ⁽⁵⁾Carreiras et al. (2006); ⁽⁶⁾Staelens
666 et al. (2006); ⁽⁷⁾Rodríguez-Calcerrada et al. (2007); ⁽⁸⁾Rodríguez and Schnabel (1998); ⁽⁹⁾Belmonte and Romero
667 (1998); ⁽¹⁰⁾Rambal et al. (2003); ⁽¹¹⁾Nagler et al. (2004); ⁽¹²⁾Llorens and Domingo (2007).

668

669

670 **TABLE 3.** Comparison between estimated (RUSLE model) and measured (¹³⁷Cs) values of soil loss in several
671 control points (n = 11) at barley fields in the Estaña catchment.

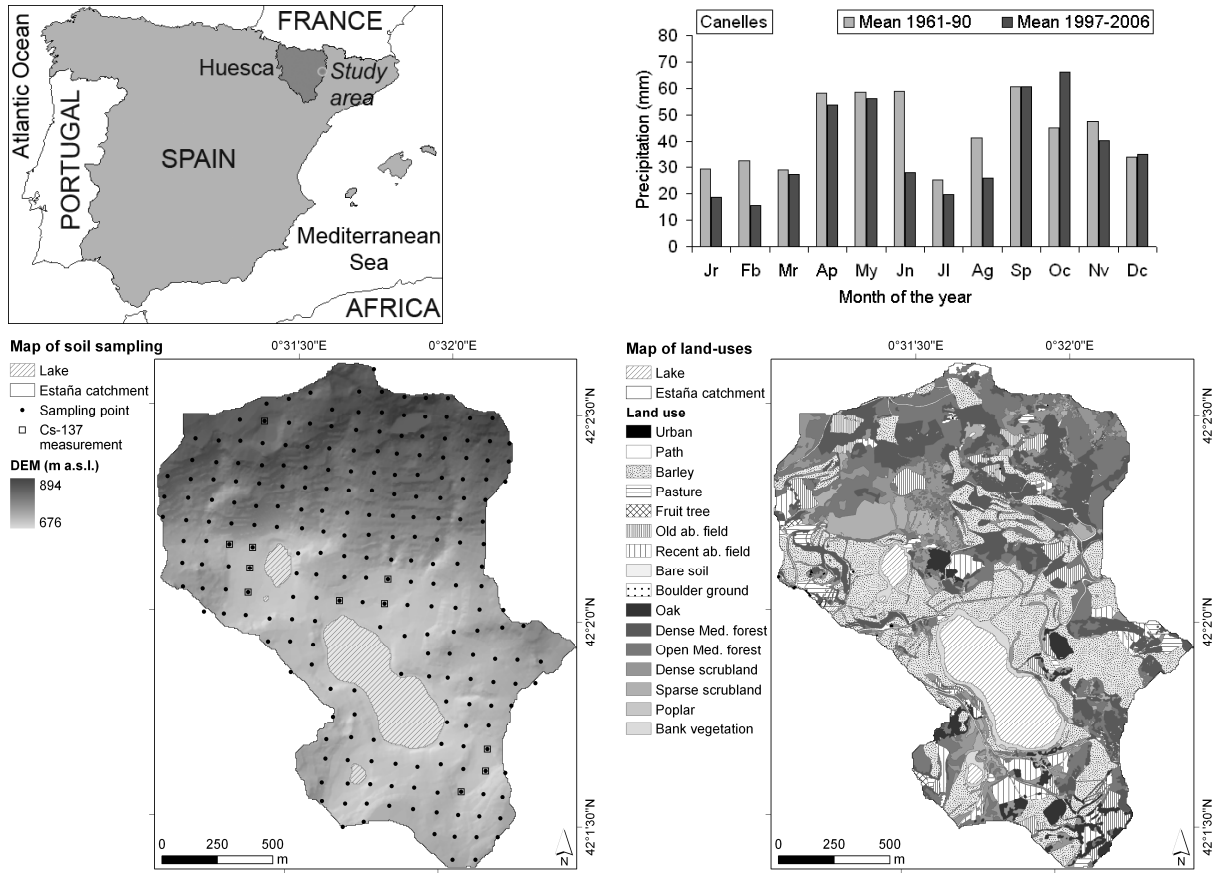
Method	A (Mg ha ⁻¹ yr ⁻¹)			
	min	max	mean	SD
RUSLE (K-texture)	0.9	15.4	3.9	4.5
RUSLE (K-K _{fs})	0.6	15.4	3.9	4.5
RUSLE (K-K _{fs} -rocks)	0.6	15.4	4.0	4.5
¹³⁷ Cs	0.9	10.5	4.9	3.4

672

TABLE 4. Statistic values of annual soil loss for the different land-uses at the Estaña catchment.

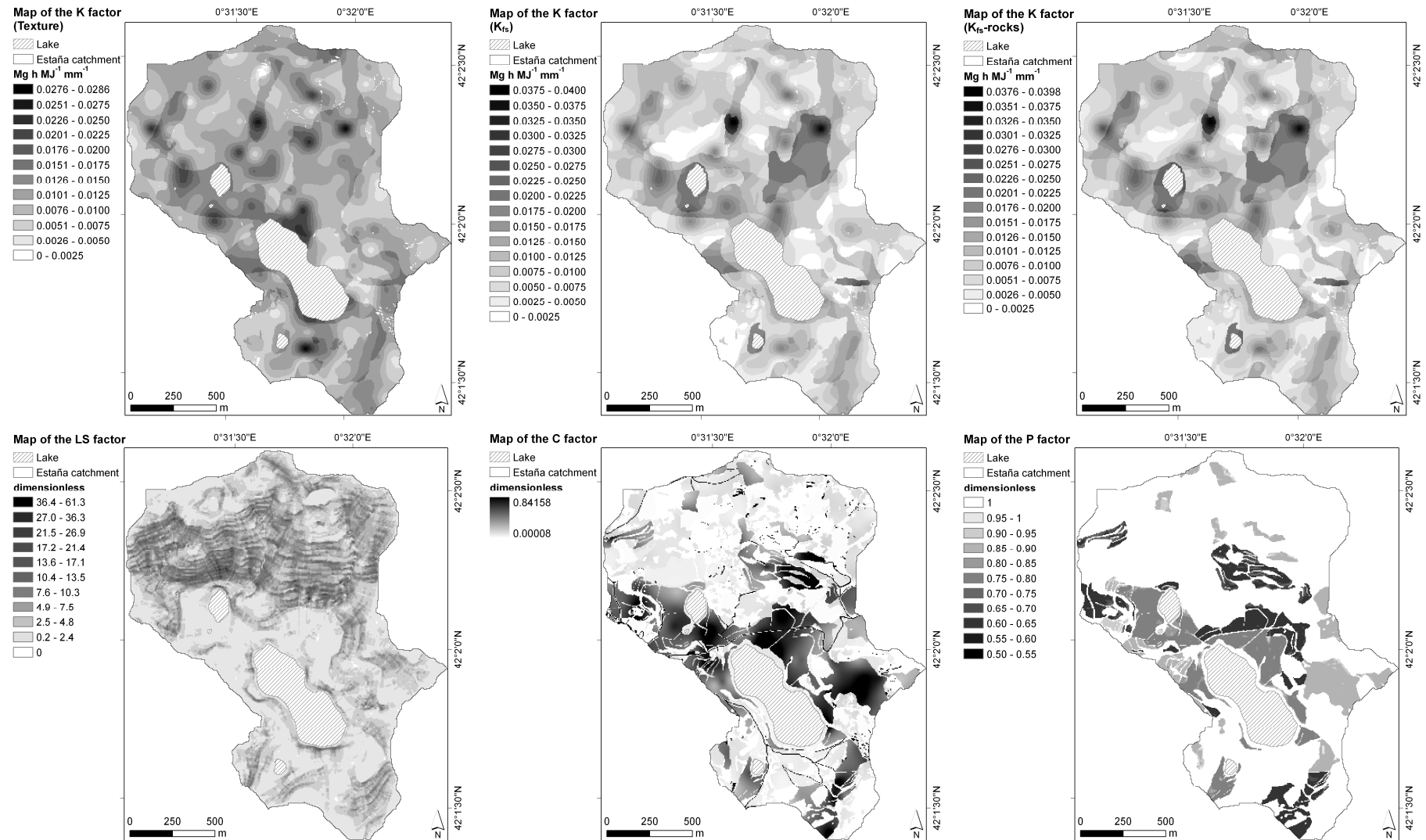
Land-use and land-cover type		K (K_{fs} -rocks)	LS	C	P	A				Total annual soil loss	
		($Mg\ h\ MJ^{-1}\ mm^{-1}$)	(-)	(-)	(-)	(Mg ha ⁻¹ yr ⁻¹)				(Mg yr ⁻¹)	(% of total)
		mean	mean	mean	mean	min	max	mean	SD		
Anthropogenic Use	Paths	0.0088	3.7	0.5027	1	0	306.3	18.7	34.4	23856	11.4
	Barley	0.0107	3.3	0.1841	0.76	0	183.7	5.0	7.8	129772	61.9
	Pasture	0.0097	3.7	0.0008	0.98	0	0.3	< 0.1	< 0.1	64	< 0.1
	Olive and almond trees	0.0076	3.0	0.0422	1	0	9.5	1.1	1.6	476	0.2
	Old abandoned fields	0.0095	6.6	0.0011	1	0	1.5	0.1	0.1	366	0.2
	Recent abandoned fields	0.0104	4.6	0.0213	1	0	13.4	1.1	1.4	4177	2.0
Natural vegetation	Oak forest	0.0093	3.1	0.0013	1	0	0.4	< 0.1	< 0.1	139	0.1
	Dense Med. forest	0.0106	6.0	0.0012	1	0	1.5	0.1	0.1	1603	0.8
	Open Med. forest	0.0090	6.1	0.0320	1	0	48.6	2.1	3.1	34434	16.4
	Dense scrubland	0.0098	6.0	0.0002	1	0	0.2	< 0.1	< 0.1	123	0.1
	Disperse scrubland	0.0085	10.6	0.0170	1	0	13.7	1.5	1.4	7054	3.4
	Poplar	0.0145	6.0	0.0005	1	0	0.2	< 0.1	< 0.1	7	< 0.1
	Bank vegetation	0.0148	2.7	0.0170	1	0	7.2	0.6	0.8	1255	0.6
	Pine woodland	0.0094	3.3	0.0006	1	0	0.1	< 0.1	< 0.1	5	< 0.1

675 **FIG. 1.** Geographic situation of the study area in the province of Huesca (Spain). Average values of monthly
 676 rainfall at the weather station of Canelles. Map of sampling points and land-uses of the Estaña catchment.

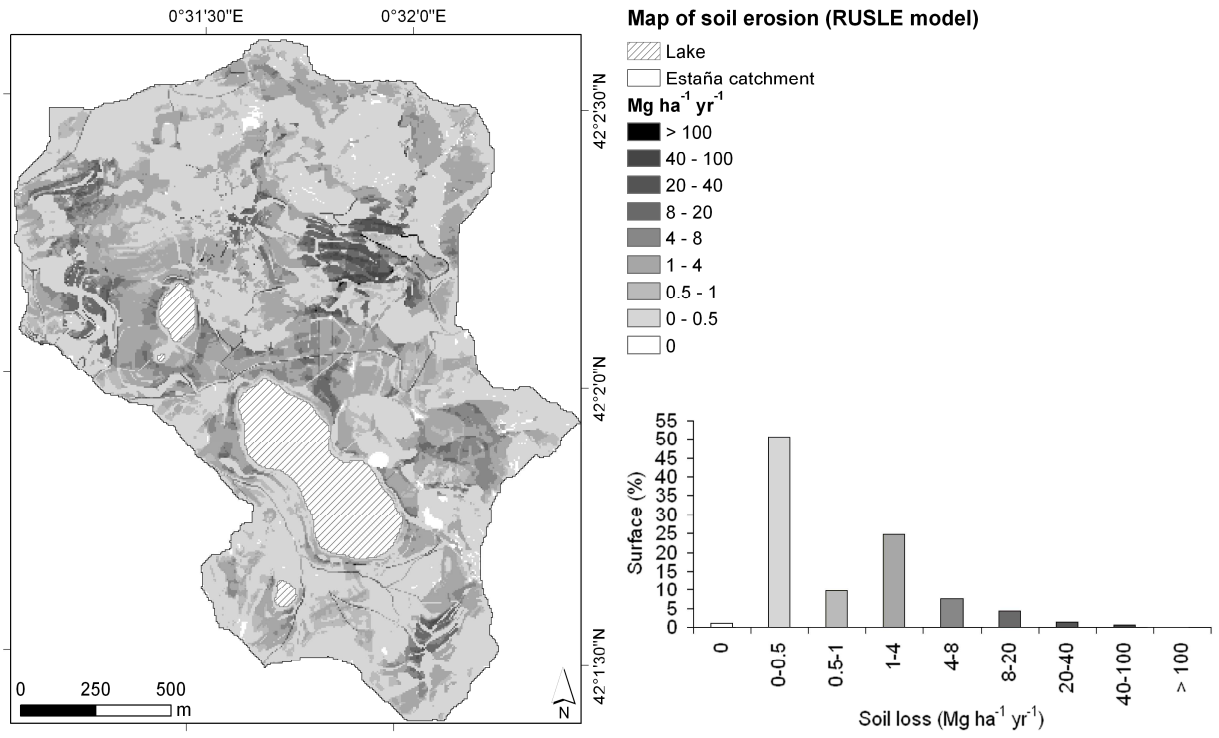


677

678

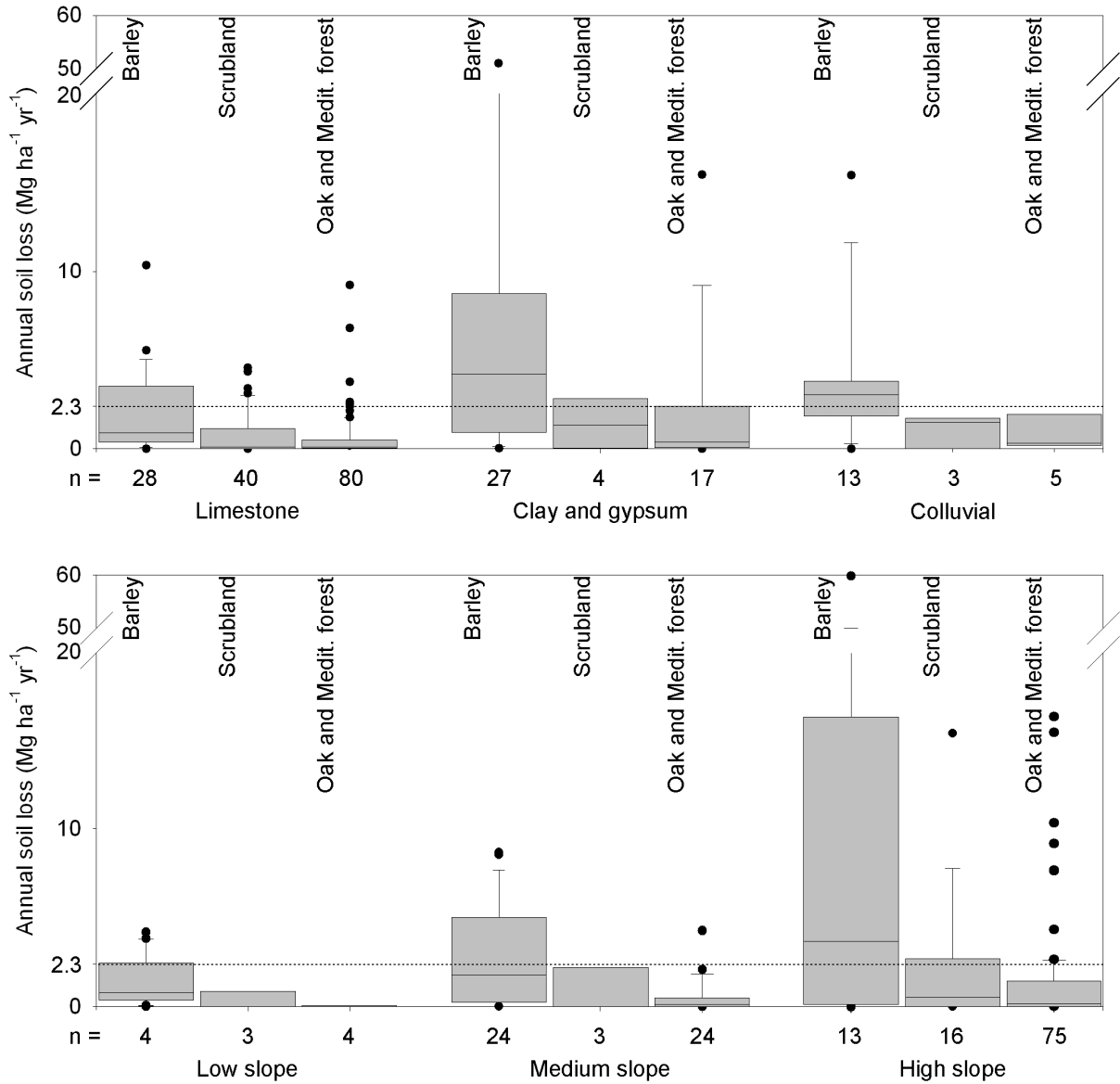
FIG. 2. Maps of the RUSLE factors of K -texture, K - K_s , K - K_{fs} -rocks, LS , C and P at the Estaña catchment.


680 **FIG. 3.** Map and histogram of predicted soil erosion with the RUSLE model at the Estaña catchment.



681
682

683 **FIG. 4.** Variation of the estimated values of soil loss at sampling points for barley fields, recently and old
 684 abandoned fields, scrublands and oak and Mediterranean forest in relation with the three main types of lithology
 685 and with different ranges of slope and orientation at the Estaña catchment.



686

687